

 Open access • Journal Article • DOI:10.1021/JM400115K

Design, Synthesis, and Inhibitory Activity of Potent, Photoswitchable Mast Cell Activation Inhibitors — [Source link](#)

Willem A. Velema, Marco van der Toorn, Wiktor Szymanski, Bernard Feringa

Published on: 13 Jun 2013 - Journal of Medicinal Chemistry (American Chemical Society)

Topics: Antiallergic agent

Related papers:

- [Reversible Photocontrol of Biological Systems by the Incorporation of Molecular Photoswitches](#)
- [Optical control of antibacterial activity](#)
- [Photopharmacology: Beyond Proof of Principle](#)
- [Photoisomerization in different classes of azobenzene](#)
- [Azobenzene photoswitches for biomolecules.](#)

Share this paper:    

View more about this paper here: <https://typeset.io/papers/design-synthesis-and-inhibitory-activity-of-potent-2peylswwdj>

University of Groningen

Design, Synthesis, and Inhibitory Activity of Potent, Photoswitchable Mast Cell Activation Inhibitors

Velema, Willem A.; van der Toorn, Marco; Szymanski, Wiktor; Feringa, Ben L.

Published in:
Journal of Medicinal Chemistry

DOI:
[10.1021/jm400115k](https://doi.org/10.1021/jm400115k)

IMPORTANT NOTE: You are advised to consult the publisher's version (publisher's PDF) if you wish to cite from it. Please check the document version below.

Document Version
Publisher's PDF, also known as Version of record

Publication date:
2013

[Link to publication in University of Groningen/UMCG research database](#)

Citation for published version (APA):

Velema, W. A., van der Toorn, M., Szymanski, W., & Feringa, B. L. (2013). Design, Synthesis, and Inhibitory Activity of Potent, Photoswitchable Mast Cell Activation Inhibitors. *Journal of Medicinal Chemistry*, 56(11), 4456-4464. <https://doi.org/10.1021/jm400115k>

Copyright

Other than for strictly personal use, it is not permitted to download or to forward/distribute the text or part of it without the consent of the author(s) and/or copyright holder(s), unless the work is under an open content license (like Creative Commons).

The publication may also be distributed here under the terms of Article 25fa of the Dutch Copyright Act, indicated by the "Taverne" license. More information can be found on the University of Groningen website: <https://www.rug.nl/library/open-access/self-archiving-pure/taverne-amendment>.

Take-down policy

If you believe that this document breaches copyright please contact us providing details, and we will remove access to the work immediately and investigate your claim.

Downloaded from the University of Groningen/UMCG research database (Pure): <http://www.rug.nl/research/portal>. For technical reasons the number of authors shown on this cover page is limited to 10 maximum.

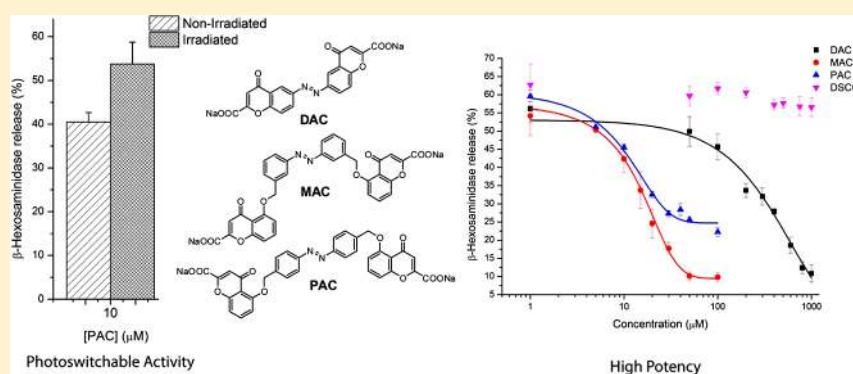
Design, Synthesis, and Inhibitory Activity of Potent, Photoswitchable Mast Cell Activation Inhibitors

Willem A. Velema,[†] Marco van der Toorn,[‡] Wiktor Szymanski,^{*,†} and Ben L. Feringa^{*,†}

[†]Centre for Systems Chemistry, Stratingh Institute for Chemistry, University of Groningen, Nijenborgh 4, 9747 AG Groningen, The Netherlands

[‡]Laboratory of Allergology and Pulmonary Diseases, Department of Pathology and Medical Biology, University Medical Centre Groningen, 9713 GZ Groningen, The Netherlands

Supporting Information



ABSTRACT: Allergic reactions affect millions of people worldwide. The need for new and effective antiallergic agents is evident, and insight into the underlying mechanisms that lead to allergic events is necessary. Herein, we report the design, synthesis, and activity of photoswitchable mast cell activation inhibitors. In mast cell degranulation assays, these inhibitors possess significantly greater potency than an original, chromone-based antiallergic agent. Furthermore, one of the photoswitchable inhibitors shows a significant difference in inhibitory activity between its two photoisomeric forms. Further optimization could ultimately lead to a photoswitchable compound suitable for studying mechanisms involved in allergic reactions in a novel manner, with activity addressable by light and with precise spatiotemporal control over events at the molecular level.

INTRODUCTION

The prevalence of allergic diseases has increased over the last decades,^{1,2} and the search for suitable pharmacotherapeutic treatment is ongoing.^{3,4} Several options to treat allergic patients are available,⁵ including antihistamines, leukotriene inhibitors, corticoids, and chromones. This last class of drugs has lost popularity, mainly due to their less pronounced effect and short duration of action.⁶ However, chromones show few side effects,⁶ as opposed to the commonly used corticoids,^{7,8} which renders them continuously interesting therapeutic agents. Furthermore, they seem to have an interesting, yet not fully understood, mechanism of action.⁹

Chromones stabilize mast cells,¹⁰ which are effector cells of immediate hypersensitivity reactions and therefore play a key role in allergic diseases.¹¹ These cells can be found throughout the human body, and they secrete granules upon activation.^{12,13} The granules contain inflammatory mediators, which induce the symptoms of an allergic reaction, like edema, warmth, and itchiness.¹² Activation of mast cells occurs as a result of cross-linking of high affinity IgE receptors on the cell surface by allergens.¹⁴ Chromones bind to the cromolyn binding protein (CBP) on the surface of mast cells and inhibit this activation

process.¹⁵ While the exact mechanism of their action is yet to be elucidated, and other targets have been proposed, it is hypothesized that chromones interfere with the calcium influx, which is necessary for degranulation.^{16,17}

Our aim was to design and synthesize a new class of chromone derivatives which have higher potency than the available, chromone-based drugs such as disodium cromoglycate¹⁸ (DSCG, Figure 1A). DSCG inhibits mast cell activation, and its structure–activity relationships are well studied.¹⁹ The drug is a dimeric ligand and consists of two chromone moieties linked by a spacer (Figure 1A). Altering the length of the spacer changes the inhibitory activity of the drug.^{19,20} However, we expected that the molecular structure of the spacer, rather than length only, might also influence the drugs' activity as was shown before, for example, for opioid receptor antagonists.²⁰ To investigate this, three different DSCG derivatives were designed with an azobenzene photoswitch as a spacer (Figure 1A). Azobenzene molecules can be photoisomerized, changing the molecule's length, dipole moment, and geometry in a

Received: January 24, 2013

Published: April 25, 2013

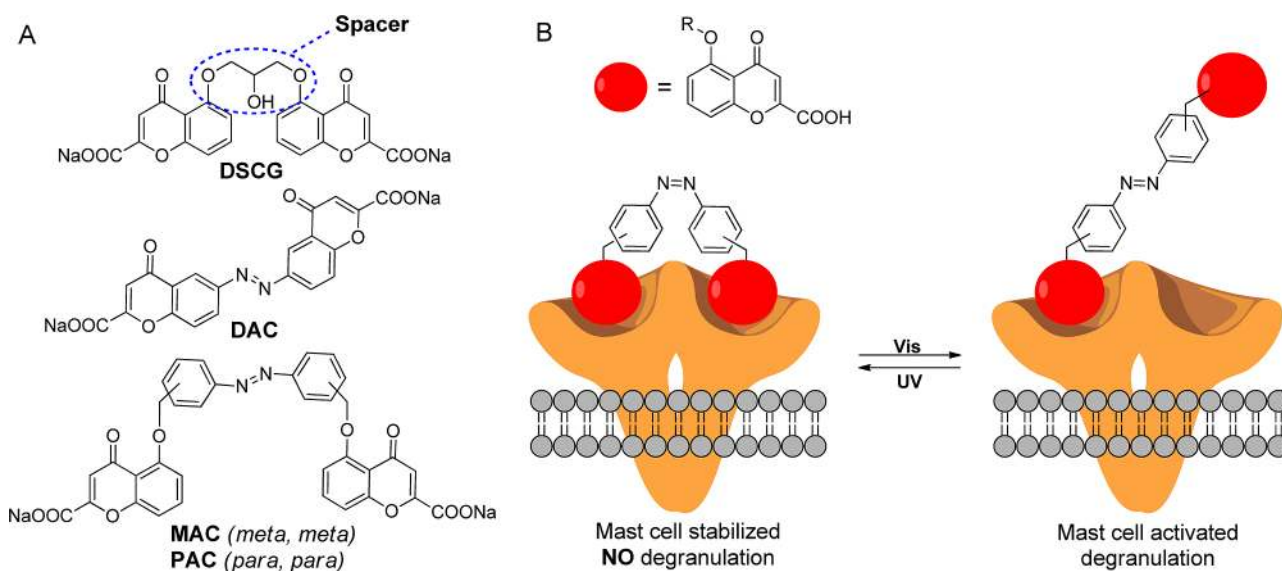
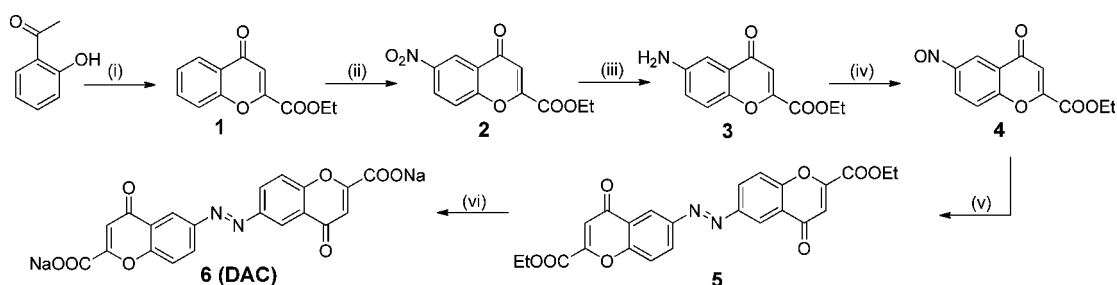


Figure 1. Principle and molecular structure of photoswitchable mast cell activation inhibitors. (A) Molecular structure of the mast cell activation inhibitor disodium cromoglycate (DSCG) and the three designed photoswitchable inhibitors DAC, MAC and PAC. (B) Envisioned mode of action of MAC and PAC. When two chromone groups (illustrated as red spheres) of the inhibitor in one of the photoisomeric forms are bound to the cromolyn binding protein (CBP), mast cell activation is inhibited. When the molecule photoisomerizes to the other form, only one chromone group can bind and mast cell activation is not inhibited.

Scheme 1^a



^aReagents and conditions: (i) diethyl oxalate, NaOEt/EtOH, HCl (75%); (ii) H₂SO₄, HNO₃, rt, 1 h (81%); (iii) H₂, Pd/C, benzene, rt, 16 h (75%); (iv) oxone, DCM/water, rt, 2 h (70%); (v) compound 3, glacial AcOH, rt, 2 d (43%); (vi) EtOH, NaOH, reflux, 2 h (91%).

reversible manner.²¹ In addition, their structure is essentially different from that of the spacer of DSCG. This allows studying the influence of both the structure and the length of the spacer on inhibitory activity of the drug. Moreover, incorporating a photoswitch into the DSCG molecule might allow changing its inhibitory potency upon light irradiation. This eventually could lead to optical control over mast cell activation with high spatiotemporal resolution, as was shown with other bioactive compounds.^{22,23} The information gained from these experiments could provide more insight into the mechanisms by which DSCG inhibits mast cell activation and the way it interacts with the CBP.

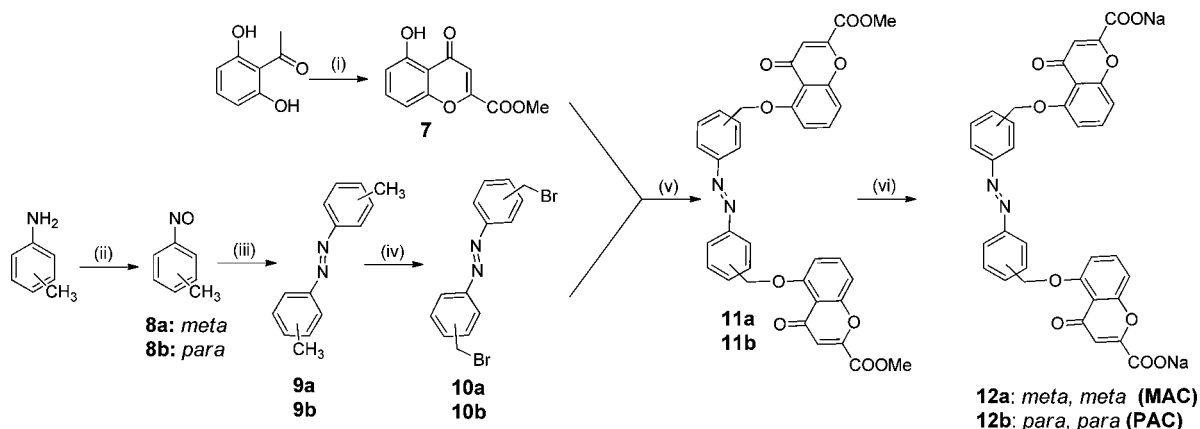
Here we present the design and synthesis of three analogues of DSCG, with an azobenzene photoswitch incorporated in their structure. The inhibitory capacity of the molecules, named diazochromone (DAC), *meta*-azochromone (MAC), and *para*-azochromone (PAC) (Figure 1A), in both photoisomeric forms was tested on human mast cell cultures. Remarkably, the molecules showed to have a considerably higher inhibitory effect on an evoked degranulation in mast cell cultures, as compared to the common drug DSCG. Furthermore, PAC showed a significant difference in inhibitory capacity in two isomeric forms. It is anticipated that external control of mast

cell activation can be achieved by switching between the two forms with light

RESULTS

Design of Photoswitchable Inhibitors. The structure of photoswitchable inhibitors DAC, MAC, and PAC was inspired by the known mast cell activation inhibitor DSCG. This drug consists of two chromone groups linked by a spacer (Figure 1A). The length of the spacer influences the inhibitory activity of the drug.¹⁹ We chose an azobenzene unit as the photoswitch to connect the chromone units because the difference in structure and length between the two forms (the *trans* and *cis* isomer) of this photoswitch is well-defined and relatively large.^{21,24} Azobenzenes are privileged photoswitches for usage in bioactive compounds for their small size and stability in aqueous environments.²¹

We hypothesized that both chromone groups need to bind to the CBP for the drug to have an optimal inhibitory effect (Figure 1B), as was shown for other bivalent compounds.^{25,26} With this in mind, we designed three photoswitchable inhibitors called DAC, MAC, and PAC (Figure 1A). The first photoswitchable inhibitor, DAC, was designed in such a way that the azobenzene photoswitch intergrates two chromone

Scheme 2^a

^aReagents and conditions: (i) dimethyl oxalate, NaOMe/MeOH, HCl (33%); (ii) oxone, DCM/water, rt, 1 h (8a, 54%; 8b, 25%); (iii) *m/p*-toluidine, glacial AcOH, rt, 16 h (9a, 55%; 9b, 86%); (iv) NBS, AIBN, CCl₄, reflux, 16 h (10a, 35%; 10b, 42%); (v) Cs₂CO₃, MeCN, reflux, 5 h (11a, 70%; 11b, 35%); (vi) EtOH, NaOH, reflux, 2 h (12a, 86%; 12b, 91%).

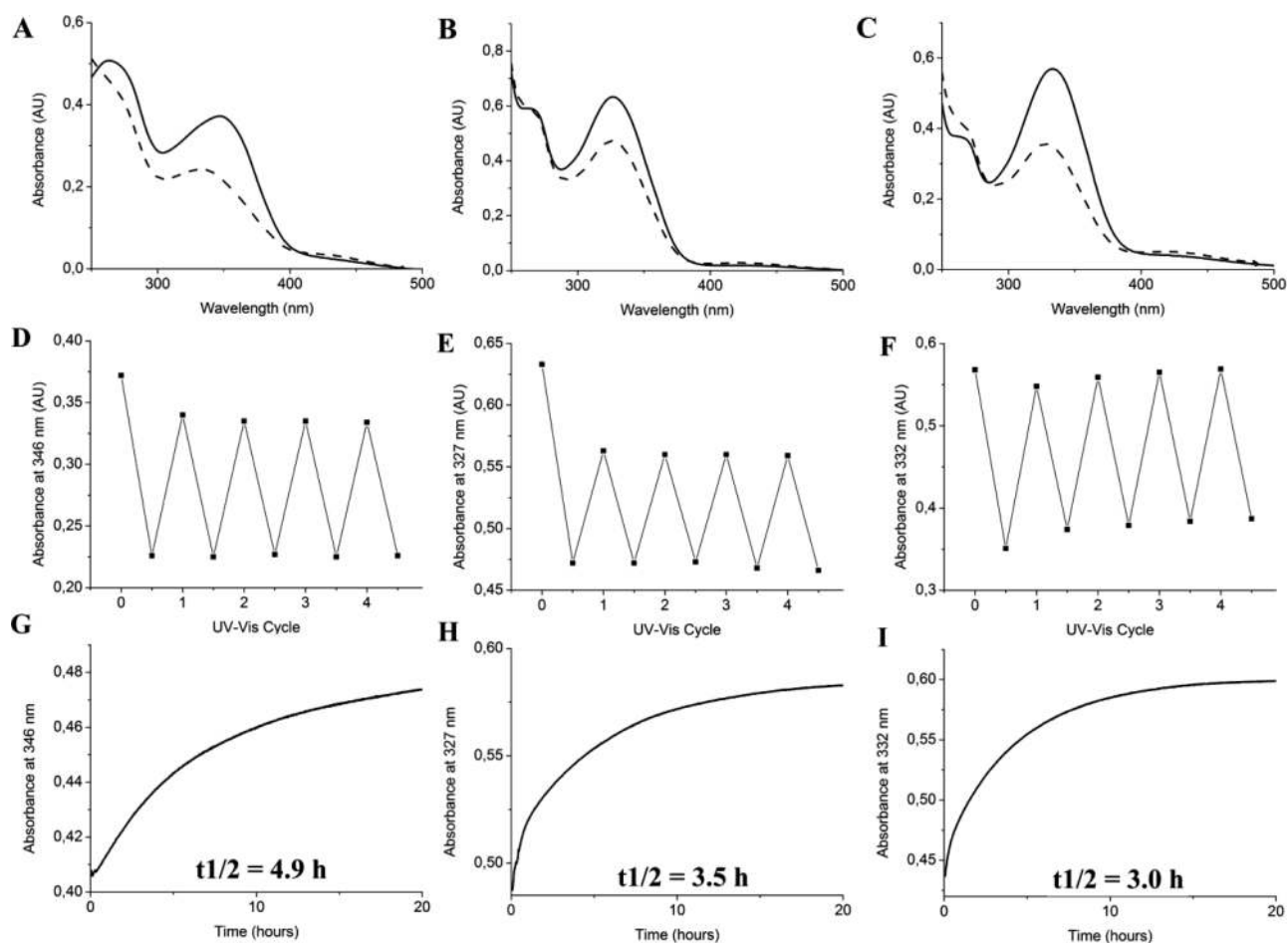


Figure 2. Photochemical properties of compounds DAC, MAC and PAC. (A–C) UV–vis absorption spectra of DAC (125 μ M), MAC (128 μ M), and PAC (100 μ M) in water. The solid lines represent the spectra of the nonirradiated forms and the dashed lines of the 365 nm irradiated forms. (D–F) Reversible photochromism of photoswitchable inhibitors. (G–I) Thermal *cis*–*trans* isomerization at 37 °C.

groups in its structure. This reduced the length of the spacer as compared to DSCG and rendered the molecule more rigid, which could result in a larger difference in inhibitory activity between the two photoisomeric forms. Compounds MAC and PAC (Figure 1A) consist of an azobenzene moiety with two chromone groups linked to it in the *meta* and *para* positions,

respectively. A methylene group was placed in between the azobenzene and chromone groups to introduce more flexibility in the molecule. This flexibility might be favorable when two chromone groups need to interact with the CBP at the same time (Figure 1B).

Synthesis. The photoswitchable inhibitor DAC was synthesized starting from chromone ethyl ester (**1**) (Scheme 1), which was obtained from hydroxyacetophenone and diethyl oxalate.²⁵ Compound **1** was converted into nitroso-chromone **4** via sequential nitration,²⁸ reduction,²⁸ and oxidation reactions. Azobenzene formation from precursors **3** and **4** and a subsequent saponification step afforded the photoswitchable inhibitor DAC (**6**).

Compounds MAC and PAC were prepared in six steps as depicted in Scheme 2. The key features of these syntheses include a formation of a diazo compound by a reaction between *m/p*-toluidine and *m/p*-nitrosotoluene (**8a** and **8b**) to afford methylated azobenzenes (**9a** and **9b**), which were subjected to radical bromination to yield compounds **10a** and **10b**. Via a double Williamson ether formation, 5-hydroxychromone methyl ester **7**, obtained from 1,2-dihydroxyacetophenone and dimethyl oxalate,²⁹ was introduced to both methylene groups of the azobenzenes **10a** and **10b**, resulting in **11a** and **11b**. A saponification step afforded the sodium salts of the photoswitchable inhibitors MAC (**12a**) and PAC (**12b**).

Photoswitching of Designed Mast Cell Activation Inhibitors. The photoswitchable behavior of DAC, MAC, and PAC was studied using UV–vis spectroscopy and RP-HPLC. The *trans*-isomers of DAC, MAC, and PAC have a characteristic absorbance maximum between 300 and 400 nm in water. This absorbance maximum decreases when the molecules are photoswitched to their *cis*-isomers and a new absorbance maximum appears around 430 nm (Figure 2A–C).³⁰ Isosbestic points at 405 nm (DAC), 270 nm (MAC), and 270 nm (PAC) clearly illustrate the selective isomerization and reversibility of the photoswitching process. Using RP-HPLC, the ratio of photoisomers was determined for both the nonirradiated and 365 nm irradiated forms of DAC, MAC, and PAC (Table 1).

Table 1. Ratio of *trans* and *cis* Isomers of the Photoswitchable Inhibitors under Different Conditions^a

	DAC (<i>trans:cis</i>)	MAC (<i>trans:cis</i>)	PAC (<i>trans:cis</i>)
nonirradiated	99:1	88:12	91:9
irradiated (water)	59:41	45:55	56:44
irradiated (DMSO)	48:52	38:62	19:81

^aRatios are determined at the isosbestic point (405 nm for DAC, 270 nm for MAC, 270 nm for PAC) with RP-HPLC (C18, flow 1 mL/min, MeCN and H₃PO₄ pH = 3.0).

Higher photostationary states were obtained when the photoswitchable inhibitors were irradiated with 365 nm light in DMSO as compared to water (Table 1). Therefore, for inhibitory activity studies (vide infra), the compounds were switched at a high concentration in DMSO and diluted in water to obtain a maximum concentration of 1% DMSO (v/v). The inhibitors could be photoisomerized by alternating irradiation at 365 nm and 400–700 nm for at least five times, showing little fatigue (Figure 2D–F). Thermal *cis*–*trans* isomerization was relatively slow at 37 °C ($t_{1/2} \geq 3$ h for all compounds) (Figure 2G–I). Because in the inhibitory activity studies (vide infra) the incubation times were only 30 min, assaying the activity of the *cis*-form without significant *cis*–*trans* conversion was possible.

Inhibitory Activity. The inhibitory activity of DAC, MAC, and PAC was determined on the LAD2³¹ mast cell line using a β -hexosaminidase release assay.³² β -Hexosaminidase is an enzyme that is secreted by mast cells upon activation, and

therefore its activity is a reliable measure for the degree of mast cell degranulation.³³ LAD2 cells were incubated with different concentrations of DSCG and nonirradiated DAC, MAC, and PAC for 30 min, after which degranulation was evoked by the secretagogue compound 48/80.³⁴ From Figure 3A, it is apparent that DAC, MAC, and PAC show significantly greater inhibitory activity than the original drug DSCG. MAC and PAC seem to have an almost 100 times greater inhibitory potency than DSCG. Furthermore, MAC and DAC show greater efficacy than PAC.

At the concentration of compound 48/80 (1.0 μ M) that was used in this assay, DSCG did not show any inhibitory activity. At lower concentrations of compound 48/80 (0.1 μ M), DSCG was able to inhibit mast cell degranulation (Figure 3B), albeit with lower activity than MAC (~100 times).

The inhibitory activity of the most potent inhibitor, MAC, was further investigated using a histamine release assay³⁵ (Figure 4). LAD2 cells were incubated with different concentrations of DSCG and MAC for 30 min, after which a degranulation was evoked by compound 48/80. At the assayed concentrations DSCG did not show any inhibitory activity, whereas MAC completely inhibited histamine release at a concentration of 100 μ M.

Next, the difference in inhibitory activity between the two photoisomers of DAC, MAC, and PAC was determined. The inhibitory activity was measured for each compound at two concentrations that were on the steep part of the concentration response curve, because at these concentrations a possible difference in inhibitory activity is most pronounced. LAD2 cells were incubated with either nonirradiated solutions of DAC, MAC, and PAC or with solutions that were irradiated with 365 nm light prior incubation. The samples were irradiated in DMSO and diluted in water to obtain a maximum concentration of 1% DMSO (v/v). After evoking a degranulation with compound 48/80, β -hexosaminidase release was determined (Figure 5). We observed no significant difference in inhibitory activity between the irradiated and nonirradiated forms of MAC and DAC. However, a significant difference was observed between the irradiated and nonirradiated form of PAC. At a concentration of 10 μ M, the relative difference in inhibitory activity between the two forms of PAC is 25%. The nonirradiated form, which consists of 91% *trans*-PAC in the photostationary state (PSS), is more active than the irradiated form, which is 81% *cis*-PAC in the PSS.

DISCUSSION

The chromone-based drugs are an attractive and routinely used class of antiallergic agents because of their mast cell stabilizing capability and the limited side effects.⁶ The main disadvantage of this class of drugs is its low effectiveness.³⁶ The novel, azobenzene-bridged, bis-chromone compounds MAC and PAC show an almost 100 times higher potency than the chromone drug DSCG based on β -hexosaminidase release assays (Figure 3). This large increase in potency makes MAC and PAC interesting potential antiallergic agents, especially if the side effect pattern remains unchanged. Further investigation is ongoing to determine the toxicity and side effects of these compounds.

In earlier research by Hunter et al., the effect of the length of the spacer between the two chromone groups on inhibitory activity was explored.¹⁹ Inhibitors containing longer spacers, consisting of alkylene chains, showed a decrease in activity when the spacer exceeded six atoms.¹⁹ Spacer length is known

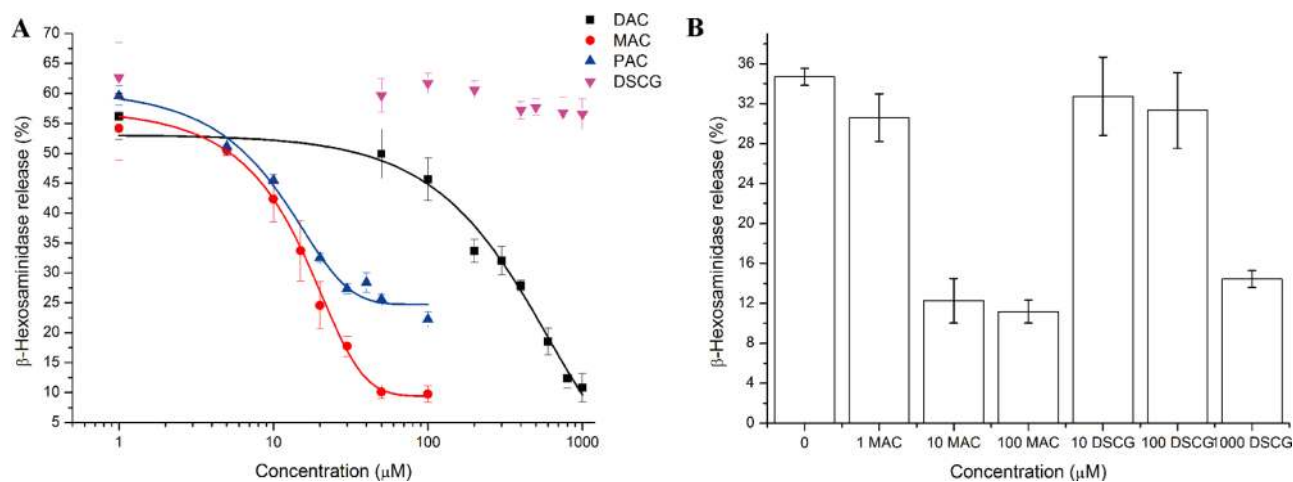


Figure 3. Concentration response curves of mast cell activation inhibitors ($n = 3$). (A) Degranulation was evoked by 1.0 $\mu\text{g}/\text{mL}$ of compound 48/80. The mast cell activation inhibitors MAC and PAC show inhibitory activity in the same concentration range with IC_{50} values of 10 and 28 μM , respectively. DAC shows to be a less potent inhibitor with an IC_{50} value of 272 μM but is still more potent than the original drug DSCG, which did not show any inhibitory activity under these conditions ($\text{IC}_{50} > 1 \text{ mM}$) (see Supporting Information Figure S1). MAC and DAC show higher efficacy than PAC. (B) Inhibitory activity of MAC and DSCG. Degranulation was evoked by 0.1 $\mu\text{g}/\text{mL}$ of compound 48/80. MAC shows complete inhibition at a concentration of 10 μM , whereas DSCG shows complete inhibition at a concentration of 1000 μM .

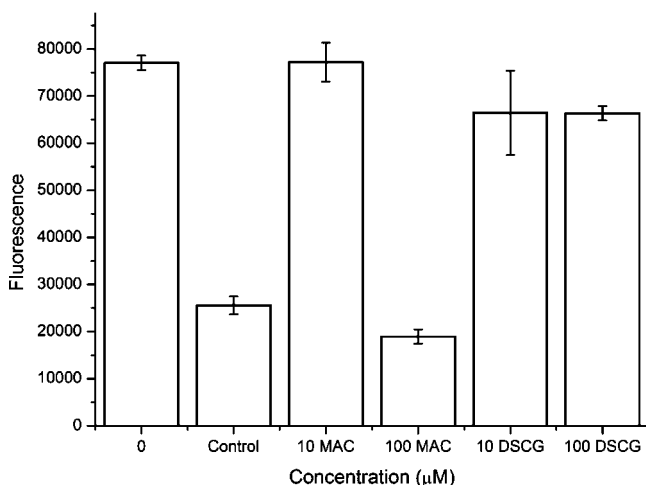


Figure 4. Histamine release assay of MAC and DSCG ($n = 3$). Degranulation was evoked by 1.0 $\mu\text{g}/\text{mL}$ of compound 48/80. MAC completely inhibited histamine release at a concentration of 100 μM . The fluorescence detected was comparable to the control measurement without compound 48/80. DSCG did not show any inhibitory activity at the studied concentrations.

to modulate selectivity in bivalent ligands.²⁰ Our results suggest that the length of the spacer plays a role in the inhibitory activity because there is a change in activity between the two isomeric forms of PAC, which have a distinct difference in distance between the chromone units. However, our results also suggest that the molecular structure of the spacer, rather than spacer length only, might be of great importance for activity. Similar observations have already been reported earlier for opioid receptor antagonists.²⁰ MAC and PAC, which include an azobenzene group as a spacer and might be considered lengthy compared to the original linker in DSCG, showed to be almost 100 times more potent than the model compound DSCG in a degranulation assay based on the activity of β -hexosaminidase released from granules.

To exclude the false positive result which could stem from the inhibition of β -hexosaminidase activity by MAC, we also assayed the amount of histamine released from the granules (Figure 4). The results obtained in this experiment confirmed the much higher activity of MAC in stabilizing mast cell activation than DSCG.

Several modes of actions for chromones have been proposed, apart from CBP binding, including the blockage of chloride channels³⁷ and G-protein-coupled-receptor 35 binding.³⁸ It is

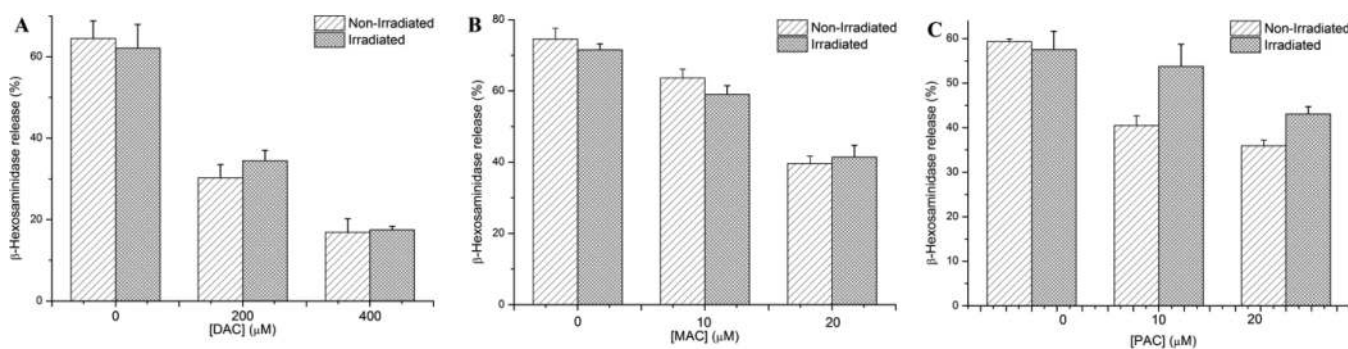


Figure 5. Inhibitory activity of the nonirradiated and 365 nm light-irradiated forms of DAC, MAC and PAC. (A,B) No difference between the two forms of DAC and MAC were observed. (C) A difference in activity was observed between the two forms of PAC. Nonirradiated PAC was 25% more active than irradiated PAC at a concentration of 10 μM .

possible that the newly designed inhibitors exhibit an effect via binding to multiple receptor types, which makes it harder to explain the effect of changes in molecular structure on activity. For instance, the effect via binding to various receptor types could provide an explanation for the observed lower efficacy of PAC, as compared to DAC, MAC, and DSCG.

The lack of difference in inhibitory activity between the two forms of MAC, which differ significantly in length, also confirms our observation that the structure and geometry of the spacer, rather than its length, is important for the interaction between mast cell activation inhibitors and the CBP.

Because there is a difference in inhibitory activity between the *cis* and *trans* isomer of PAC, this photoswitchable inhibitor might be a useful tool to study the events involved in mast cell degranulation. To completely control the state of mast cell activation as an "on/off" event, it is necessary to enhance the difference in activity between the two forms of a photoswitchable inhibitor. To achieve this, first the PSS of the least active isomer should be optimized. In case of PAC, the least active isomer is the *cis* form. The PSS of irradiated PAC consists of 81% *cis* and 19% *trans*. This means that when PAC is photoisomerized, still 19% of the more potent isomer is present. If this percentage can be reduced, a larger difference in activity would be obtained. One possibility to achieve this is the use of bidirectional azobenzenes.^{39–42} In this class of azobenzenes, the UV–vis absorption maxima of the *trans* and *cis* form do not overlap, which allows better control over photoisomerization and results in a high PSS for both forms. Second, the optimal distance between the two chromone groups in the molecular structure of the inhibitor needs to be investigated. Then a photoswitchable inhibitor could be designed with maximum activity in one photoisomeric form and minimum activity in the other form.

CONCLUSIONS

Three photoswitchable mast cell activation inhibitors have been designed and synthesized. All three inhibitors are more potent than the commercially available drug DSCG. Especially the compounds MAC and PAC show a large increase in potency when compared to DSCG, which renders them interesting candidates for antiallergic agents. Our results suggest that the molecular structure of the spacer connecting the two chromone groups is of great importance for activity. Furthermore, a difference in inhibitory activity was observed between the nonirradiated and irradiated form of PAC. This result comprises the first step on the way to our far reaching goal, i.e., obtaining complete control over mast cell activation with light. In addition, our results show how molecular photo-switches can be used to study and interfere in a noninvasive manner with biological processes and how they might be used as a tool in chemical biology.

EXPERIMENTAL SECTION

LAD2 Cell Culture. The human mast cell line LAD2 was kindly provided by Dr. A. Kirshenbaum (National Institute of Allergy and Infectious Diseases, Bethesda, MD). LAD2 cells were cultured in suspension at 37 °C, 95% relative humidity, and 5% CO₂ in StemPro-34 serum-free medium (Invitrogen) supplemented with 2 mM L-glutamine (Sigma Aldrich), 100 IU/mL penicillin (Sigma Aldrich), 100 μg/mL streptomycin (Sigma Aldrich), and 100 ng/mL rhSCF (Invitrogen). Cells were not allowed to grow beyond a density of 5.0 × 10⁵ cells/mL, and fresh medium was supplied once a week.

β-Hexosaminidase Assay. β-Hexosaminidase release was measured according to a published method.³³ In short, 50 μL of

supernatant was transferred to a 96-well plate. To this, 100 μL of a 2 mg/mL solution of *p*-nitrophenyl-*N*-acetyl-*D*-glucosaminidase in citrate buffer pH 4.5 was added. The plate was incubated at 37 °C for 1 h. The reaction was stopped by adding 100 μL of 0.4 M glycine solution, and the absorbance was measured on a fluorescent plate reader at a wavelength of 405 nm. Subsequently, the percentage of released β-hexosaminidase was determined by comparison with the absorption of cell lysate of the same cells using the following formula:

$$\frac{\text{supernatant}}{\text{supernatant} + \text{lysate}} \times 100\% = \% \text{released } \beta\text{-hexosaminidase}$$

Histamine Assay. Histamine release was measured according to a published method.³⁵ In short, 80 μL of supernatant was transferred to a 96-well plate. To this, 20 μL of a 1 M aqueous NaOH solution was added. Next, 20 μL of an 0.25% *o*-phthalaldehyde in MeOH was added and incubated for 4 min at room temperature. Then 10 μL of a 3 M aqueous HCl solution was added and the fluorescence was measured on a fluorescent plate reader ($\lambda_{\text{ex}} = 360 \text{ nm}$, $\lambda_{\text{em}} = 450 \text{ nm}$).

Inhibitory Activity Tests. LAD2 cells were suspended in HEPES buffer at a concentration of 50000 cells/mL for the β-hexosaminidase release assay and 1000000 cells/mL for the histamine release assay. Then 80 μL of cell suspension was transferred to a microreaction cup, to which 10 μL of inhibitor solution was added. This was incubated at 37 °C for 30 min, after which 10 μL of a compound 48/80 solution was added. Next, the cell suspension was incubated for 30 min at 37 °C and the β-hexosaminidase or histamine release was assayed.

Photoswitching Experiments. Irradiation experiments were performed with a spectroline ENB-280C/FE UV lamp (365 nm) and Thor Laboratories OSL1-EC fiber illuminator (white light).

Synthesis. General. For synthesis, all chemicals were obtained from commercial sources and used as received unless stated otherwise. Solvents were reagent grade. Thin-layer chromatography (TLC) was performed using commercial Kieselgel 60, F254 silica gel plates. Flash chromatography was performed on silica gel (Silicycle Siliacflash P60, 40–63 m, 230–400 mesh). Drying of solutions was performed with MgSO₄, and solvents were removed with a rotary evaporator. Chemical shifts for NMR measurements were determined relative to the residual solvent peaks. The following abbreviations are used to indicate signal multiplicity: s, singlet; d, doublet; t, triplet; q, quartet; m, multiplet; brs, broad signal; appt, apparent triplet. HRMS (ESI) spectra were obtained on a Thermo Scientific LTQ Orbitrap XL. Melting points were recorded using a Buchi melting point B-545 apparatus. UV–vis absorption spectra were recorded on an Agilent 8453 UV–visible spectrophotometer using Uvasol grade solvents. All compounds whose IC₅₀ values were determined had purities ≥95%. Purities were determined with analytical RP-HPLC performed on a JASCO PU-980 chromatography system using a GRACE Alltima HP C18 5 μm column. Compounds were detected with a JASCO UV-1575 UV–vis intelligent detector.

Ethyl 4-Oxo-4H-chromene-2-carboxylate (1). 2-Hydroxyacetophenone (2.04 g, 15 mmol) and diethyl oxalate (5.12 g, 35 mmol) were dissolved in ethanol (10 mL) and added to a solution of sodium (1.49 g, 65 mmol) in ethanol (100 mL). The reaction mixture was heated at reflux for 1 h, after which it was cooled down and acidified with concentrated HCl until a white precipitate was formed. The precipitate was filtered off, and the filtrate was concentrated and extracted with ethyl acetate, washed with brine, and dried (MgSO₄). After evaporation, a solid was obtained, which was recrystallized from methanol/di-*iso*-propylether (4:1) to yield 2.45 g (75%) of a white solid; mp 66–68 °C. ¹H NMR (400 MHz, CDCl₃): δ 8.21 (dd, *J* = 7.9, 1.7 Hz, 1H), 7.75 (ddd, *J* = 8.7, 7.1, 1.7 Hz, 1H), 7.62 (dd, *J* = 8.6, 1.0 Hz, 1H), 7.46 (ddd, *J* = 8.1, 7.1, 1.1 Hz, 1H), 7.12 (s, 1H), 4.47 (q, *J* = 7.1 Hz, 4H), 1.41 (t, *J* = 7.2 Hz, 3H). ¹H NMR spectrum in agreement with published data.²⁷

Ethyl 6-Nitro-4-oxo-4H-chromene-2-carboxylate (2). Compound 1 (200 mg, 0.92 mmol) was suspended in 65% nitric acid (0.12 mL), and the mixture was cooled on ice. Concentrated sulfuric acid (1.5 mL) was added, and the mixture was stirred for 2 h at room temperature and poured on ice-cooled water, and the formed

precipitate was filtered off to yield 195 mg (81%) of a white solid; mp 178–179 °C. ¹H NMR (400 MHz, CDCl₃): δ 9.07 (d, *J* = 2.8 Hz, 1H), 8.57 (dd, *J* = 9.2, 2.8 Hz, 1H), 7.78 (d, *J* = 9.2 Hz, 1H), 7.19 (s, 1H), 4.50 (q, *J* = 7.2 Hz, 2H), 1.46 (t, *J* = 7.1 Hz, 3H). ¹³C NMR (100 MHz, CDCl₃): δ 176.8, 159.7, 158.7, 152.8, 145.2, 128.9, 124.4, 122.5, 120.6, 115.0, 63.5, 14.1. HR-MS (ESI, [M + H]⁺): calcd for C₁₂H₁₀NO₆, 264.0508; found, 264.0502.

Ethyl 6-Amino-4-oxo-4H-chromene-2-carboxylate (3). Compound 2 (300 mg, 1.14 mmol) was dissolved in benzene (100 mL) and stirred overnight with 10% palladium on charcoal (15 mg) under a hydrogen atmosphere (balloon) at room temperature. The mixture was filtered over Celite. The filtrate was evaporated, yielding 300 mg of orange needles; mp 177–178 °C. ¹H NMR (400 MHz, CDCl₃): δ 7.45 (d, *J* = 9.0 Hz, 1H), 7.35 (d, *J* = 2.9 Hz, 1H), 7.11–7.03 (m, 2H), 4.45 (q, *J* = 7.1 Hz, 2H), 3.92 (brs, 2H), 1.43 (t, *J* = 7.1 Hz, 3H). ¹³C NMR (100 MHz, CDCl₃): δ 178.4, 160.8, 151.7, 149.6, 144.6, 125.4, 123.2, 119.8, 113.6, 107.4, 62.8, 14.1. HR-MS (ESI, [M + H]⁺): calcd for C₁₂H₁₂NO₄, 234.0766; found, 234.0762.

Ethyl 6-Nitroso-4-oxo-4H-chromene-2-carboxylate (4). Compound 3 (100 mg, 0.43 mmol) was dissolved in DCM (2 mL), a solution of oxone (422 mg, 0.69 mmol) in H₂O (8 mL) was added, and the biphasic mixture was stirred at room temperature for 2 h. The organic layer was separated, and the aqueous layer was extracted twice with DCM. The combined organic layers were washed with 1 M aq HCl, saturated NaHCO₃, and brine, and dried (MgSO₄). Evaporation of the solvent yielded 75 mg (70%) of a green solid; mp 144–145 °C. ¹H NMR (400 MHz, CDCl₃): δ 9.31 (d, *J* = 2.1 Hz, 1H), 7.77–7.65 (m, 2H), 7.21 (s, 1H), 4.50 (q, *J* = 7.1 Hz, 2H), 1.46 (t, *J* = 7.1 Hz, 3H). ¹³C NMR (100 MHz, CDCl₃): δ 177.9, 161.6, 159.9, 159.2, 152.6, 125.6, 124.9, 120.8, 120.2, 115.0, 63.4, 14.1. HR-MS (ESI, [M + H]⁺): calcd for C₁₂H₁₀NO₅, 248.0559; found, 248.0552.

Diethyl 6,6'-(Diazene-1,2-diyl)bis(4-oxo-4H-chromene-2-carboxylate) (5). Compounds 3 (70.8 mg, 0.304 mmol) and 4 (75.0 mg, 0.304 mmol) were dissolved in glacial acetic acid (2.5 mL) and stirred for 2 d. The solution was diluted with water and extracted with DCM. The organic phase was washed with water (4×) and brine and dried (MgSO₄). Recrystallization from DCM yielded 60 mg (43%) of a light-orange solid; mp 254–255 °C (dec). ¹H NMR (400 MHz, CDCl₃): δ 8.79 (d, *J* = 2.4 Hz, 2H), 8.35 (dd, *J* = 9.0, 2.4 Hz, 2H), 7.77 (d, *J* = 9.0 Hz, 2H), 7.18 (s, 2H), 4.50 (q, *J* = 7.2 Hz, 4H), 1.46 (t, *J* = 7.1 Hz, 6H). ¹³C NMR (100 MHz, CDCl₃): δ 178.1, 160.3, 157.5, 152.4, 149.4, 127.2, 125.0, 122.8, 120.2, 114.9, 63.2, 14.1. HR-MS (ESI, [M + H]⁺): calcd for C₂₅H₁₈N₂O₈, 463.1136; found, 463.1131.

Sodium (E)-6,6'-(Diazene-1,2-diyl)bis(4-oxo-4H-chromene-2-carboxylate) (6) (DAC). To a solution of compound 5 (50 mg, 0.11 mmol) in ethanol (2 mL) was added aq NaOH (2.5 M, 0.128 mL) dropwise at 0 °C. The reaction mixture was heated at reflux for 2 h, after which the insoluble product was filtered off and purified by recrystallization from methanol, yielding 45 mg (91%) of a red solid. ¹H NMR (400 MHz, methanol-*d*₄): δ 8.71 (d, *J* = 2.4 Hz, 2H), 8.43 (dd, *J* = 9.0, 2.5 Hz, 2H), 7.90 (d, *J* = 9.0 Hz, 2H), 7.04 (s, 2H). ¹³C NMR (100 MHz, methanol-*d*₄): δ 180.2, 164.2, 160.3, 157.9, 149.3, 126.7, 124.2, 121.5, 120.3, 111.1. HR-MS (ESI, [M + Na]⁺): calcd for C₂₀H₉N₂O₈Na, 451.0154; found, 451.0149.

Methyl 5-Hydroxy-4-oxo-4H-chromene-2-carboxylate (7). 2,6-Dihydroxyacetophenone (1.50 g, 9.90 mmol) and dimethyloxalate (5.80 g, 49.3 mmol) were dissolved in 0.5 M MeONa/MeOH (100 mL) and heated at reflux overnight. The solvent was removed in vacuo, and the slurry was dissolved in water (100 mL) and subsequently acidified with concentrated HCl. The precipitate was filtered off and dissolved in MeOH (50 mL) and concentrated HCl (10 mL). This solution was heated at reflux for 2 h, after which the crude product was purified by flash chromatography (Silicagel, 40–63 μm, pentane/AcOEt, 9:1, v/v), yielding 762 mg (33%) of a yellow powder. ¹H NMR (400 MHz, CDCl₃): δ 7.61 (appt, *J* = 8.4 Hz, 1H), 7.03–7.06 (m, 2H), 6.85 (d, *J* = 8.3 Hz, 1H), 4.02 (s, 3H). ¹H NMR spectrum in agreement with published data.²⁹

1-Methyl-3-nitrosobenzene (8a). 3-Methylaniline (708 mg, 6.61 mmol) was dissolved in DCM (20 mL), a solution of oxone (8.10g, 13.2 mmol) in water (80 mL) was added, and the resulting biphasic

mixture was stirred at room temperature for 30 min. The organic layer was separated, and the aqueous layer was extracted twice with DCM. The combined organic layers were washed with 1 M aq HCl, saturated NaHCO₃, and brine, and dried (MgSO₄). The crude product was purified by flash chromatography (Silicagel, 40–63 μm, pentane/AcOEt, 4:1, v/v), yielding 430 mg (54%) of a light-green solid. ¹H NMR (400 MHz, CDCl₃): δ 7.77 (d, *J* = 6.4 Hz, 1H), 7.63 (s, 1H), 7.48–7.54 (m, 2H), 2.50 (s, 3H). ¹H NMR spectrum in agreement with published data.⁴³

1-Methyl-4-nitrosobenzene (8b). 4-Methylaniline (5.00 g, 33.1 mmol) was dissolved in DCM (100 mL), a solution of oxone (40.7 g, 66.2 mmol) in water (400 mL) was added to this, and the resulting biphasic mixture was stirred at room temperature for 30 min. The organic layer was separated, and the aqueous layer was extracted twice with DCM. The combined organic layers were washed with 1 M aq HCl, saturated NaHCO₃, and brine, and dried (MgSO₄). Evaporation of the solvent yielded 2.34 g (59%) of a light-green solid. ¹H NMR (400 MHz, CDCl₃): δ 7.81 (d, *J* = 8.2 Hz, 2H), 7.39 (d, *J* = 8.0 Hz, 2H), 2.44 (s, 3H). ¹H NMR spectrum in agreement with published data.⁴⁴

3,3'-Dimethylazobenzene (9a). Compound 8a (500 mg, 4.13 mmol) and 3-methylaniline (369 mg, 3.44 mmol) were dissolved in glacial acetic acid (33 mL), and the mixture was stirred overnight. The solution was diluted with water and extracted with ethyl acetate. The organic phase was washed four times with water and once with brine and dried (MgSO₄). The crude product was filtered through silica, yielding 400 mg (55%) of an orange solid. ¹H NMR (400 MHz, CDCl₃): δ 7.70–7.74 (m, 4H), 7.41 (appt, *J* = 8.0 Hz, 2H), 7.29 (d, *J* = 7.6 Hz, 2H), 2.46 (s, 6H). ¹H NMR spectrum in agreement with published data.⁴⁵

4,4'-Dimethylazobenzene (9b). Compound 8b (300 mg, 2.48 mmol) and 4-methylaniline (292 mg, 2.73 mmol) were dissolved in glacial acetic acid (20 mL) and stirred overnight. The solution was diluted with water and extracted with ethyl acetate. The organic phase was washed four times with water and once with brine and dried (MgSO₄). The crude product was purified by flash chromatography (Silicagel, 40–63 μm, pentane/Et₂O, 9:1, v/v), yielding 450 mg (86%) of an orange solid. ¹H NMR (400 MHz, CDCl₃): δ 7.81 (d, *J* = 8.4 Hz, 4H), 7.30 (d, *J* = 8.4 Hz, 4H), 2.43 (s, 6H). ¹H NMR spectrum in agreement with published data.⁴⁶

3,3'-Bis(bromomethyl)azobenzene (10a). To a solution of compound 9a (1.30 g, 6.18 mmol) in 60 mL of CCl₄ was added NBS (2.50 g, 14.2 mmol) and AIBN (80 mg, 0.48 mmol). The resultant solution was stirred overnight at 70 °C, then filtered, and the filtrate was washed with hot water and brine and dried (MgSO₄). After evaporation the product was recrystallized from acetonitrile, yielding 800 mg (35%) of an orange solid; mp 140–141 °C. ¹H NMR (400 MHz, CDCl₃): δ 7.95 (m, 2H), 7.87 (m, 2H), 7.52 (m, 4H), 4.59 (s, 4H). ¹H NMR spectrum in agreement with published data.⁴⁵

4,4'-Bis(bromomethyl)azobenzene (10b). To a solution of compound 9b (300 mg, 1.43 mmol) in 20 mL of CCl₄ was added NBS (584 mg, 3.30 mmol) and AIBN (18 mg, 0.10 mmol). The resultant solution was stirred overnight at 70 °C, then filtered, and the filtrate was washed with hot water and brine and dried (MgSO₄). After evaporation of the solvent, the product was recrystallized from acetonitrile, yielding 220 mg (42%) of an orange solid; mp 183–185 °C. ¹H NMR (400 MHz, CDCl₃): δ 7.89 (d, *J* = 8.4 Hz, 4H), 7.54 (d, *J* = 8.4 Hz, 4H), 4.56 (s, 4H). ¹H NMR spectrum in agreement with published data.⁴⁶

(E)-Dimethyl5,5'-(((diazene-1,2-diyl)bis(3,1-phenylene))bis(methylene))bis(oxy))bis(4-oxo-4H-chromene-2-carboxylate) (11a). To a solution of compounds 7 (638 mg, 2.73 mmol) and 10a (400 mg, 1.09 mmol) in 80 mL of acetonitrile was added K₂CO₃ (452 mg, 3.27 mmol), and the resulting mixture was stirred overnight at 65 °C. The solution was concentrated in vacuo, and the crude product was purified using flash chromatography (Silicagel, 40–63 μm, DCM/methanol, 95:5, v/v), yielding 520 mg (70%) of a light-orange solid. ¹H NMR (400 MHz, CDCl₃): δ 8.06 (s, 2H), 7.90–7.85 (m, 4H), 7.56–7.61 (m, 4H), 7.18 (d, *J* = 8.5 Hz, 2H), 7.02 (s, 2H), 6.91 (d, *J* = 8.3 Hz, 2H), 5.38 (s, 4H), 4.00 (s, 6H). ¹³C NMR (100 MHz,

CDCl₃): δ 177.6, 161.1, 158.4, 158.0, 152.7, 150.1, 137.5, 134.7, 129.7, 129.4, 122.6, 120.7, 116.7, 113.8, 111.1, 108.9, 70.6, 53.4. HR-MS (ESI, [M + H]⁺): calcd for C₃₆H₂₇N₂O₁₀, 647.1660; found, 647.1603.

(*E*-Dimethyl5,5'-(((Diazene-1,2-diylbis(4,1-phenylene))bis(methylene))bis(oxy))bis(4-oxo-4H-chromene-2-carboxylate) (**11b**).

To a solution of compounds **7** (100 mg, 0.45 mmol) and **10b** (75.8 mg, 0.21 mmol) in acetonitrile (25 mL) was added Cs₂CO₃ (201 mg, 0.62 mmol), and the resulting mixture was stirred at 65 °C for 3 h. The solution was concentrated in vacuo, and the residue was dissolved in DCM, washed with 1 M aq HCl, saturated NaHCO₃, and brine, and dried (MgSO₄). After evaporation, the product was recrystallized from DCM yielding 27 mg of a light-orange solid; mp 235–237 °C (dec). ¹H NMR (400 MHz, CDCl₃): δ 7.96 (d, *J* = 8.0 Hz, 4H), 7.76 (d, *J* = 8.1 Hz, 4H), 7.58 (t, *J* = 8.0, 2H), 7.18 (d, *J* = 8.2 Hz, 2H), 7.02 (s, 2H), 6.90 (d, *J* = 8.3 Hz, 2H), 5.36 (s, 4H), 4.00 (s, 6H). ¹³C NMR (100 MHz, CDCl₃): δ 177.7, 161.1, 158.4, 158.0, 152.2, 150.1, 139.3, 134.6, 127.2, 123.2, 116.6, 113.8, 111.1, 108.7, 70.5, 53.4. HR-MS (ESI, [M + H]⁺): calcd for C₃₆H₂₇N₂O₁₀, 669.1485; found, 669.1480.

Sodium (*E*-5,5'-(((Diazene-1,2-diylbis(3,1-phenylene))bis(methylene))bis(oxy))bis(4-oxo-4H-chromene-2-carboxylate) (**12a**) (MAC). To a solution of compound **11a** (100 mg, 0.15 mmol) in ethanol (5 mL) was added aq NaOH (2.5 M, 186 μ L) dropwise at 0 °C. The reaction mixture was heated at reflux for 2 h, after which the insoluble product was filtered off, yielding 85 mg (86%) of an orange solid. ¹H NMR (400 MHz, methanol-*d*₄): δ 8.12 (s, 2H), 7.86 (d, *J* = 8.0 Hz, 2H), 7.81 (d, *J* = 8.0 Hz, 2H), 7.63 (m, 4H), 7.26 (d, *J* = 8.4 Hz, 2H), 7.06 (d, *J* = 8.4 Hz, 2H), 6.88 (s, 2H), 5.42 (s, 4H). ¹³C NMR (100 MHz, methanol-*d*₄): δ 180.4, 164.7, 158.3, 158.1, 157.9, 152.7, 138.3, 134.5, 129.1, 121.2, 113.8, 112.5, 110.9, 108.5, 69.9. HR-MS (ESI, [M + Na]⁺): calcd for C₃₄H₂₂N₂O₁₀Na, 641.1167; found, 641.1140.

Sodium (*E*-5,5'-(((Diazene-1,2-diylbis(4,1-phenylene))bis(methylene))bis(oxy))bis(4-oxo-4H-chromene-2-carboxylate) (**12b**) (PAC). To a solution of compound **11b** (25 mg, 0.04 mmol) in ethanol (3 mL) was added aq NaOH (2.5 M, 50 μ L) dropwise at 0 °C. The reaction mixture was heated at reflux for 2 h, after which the insoluble product was filtered off, yielding 23 mg (91%) of an orange solid. ¹H NMR (400 MHz, methanol-*d*₄): δ 7.96 (d, *J* = 8.3 Hz, 4H), 7.80 (d, *J* = 8.2 Hz, 4H), 7.67 (t, *J* = 8.4 Hz, 2H), 7.28 (d, *J* = 8.5 Hz, 2H), 7.05 (d, *J* = 8.3 Hz, 2H), 6.89 (s, 2H), 5.41 (s, 4H). ¹³C NMR (100 MHz, methanol-*d*₄): δ 180.3, 164.6, 158.3, 158.1, 158.0, 155.8, 152.1, 140.2, 134.4, 127.3, 122.5, 112.5, 110.9, 108.4, 69.8. HR-MS (ESI, [M + Na]⁺): calcd for C₃₄H₂₂N₂O₁₀Na, 641.1167; found, 641.1155.

■ ASSOCIATED CONTENT

Supporting Information

β -Hexosaminidase release assay of DSCG. This material is available free of charge via the Internet at <http://pubs.acs.org>.

■ AUTHOR INFORMATION

Corresponding Author

*Phone: +31 50 363 4235. Fax: +31 50 363 4296. E-mail: b.l.feringa@rug.nl (B.L.F.); w.c.szymanski@rug.nl (W.S.).

Notes

The authors declare no competing financial interest.

■ ACKNOWLEDGMENTS

We would like to thank Dr. A. Kirshenbaum and Yun Bai (National Institute of Allergy and Infectious Diseases, Bethesda, MD) for kindly providing us with the LAD2 cell line and for their help with the β -hexosaminidase release assay. This work was financially supported by the European Research Council (ERC) advanced grant 227897 to B.L.F. and by the Ministry of Education, Culture and Science (Gravity program 024.001.035).

■ ABBREVIATIONS USED

CBP, cromolyn binding protein; DSCG, disodium cromoglycate; DAC, di-azochromone; MAC, meta-azochromone; PAC, para-azochromone; PSS, photostationary state; rhSCF, recombinant human stem cell factor

■ REFERENCES

- (1) Sly, R. M. Changing prevalence of allergic rhinitis and asthma. *Ann. Allergy Asthma Immunol.* **1999**, *28*, 233–248.
- (2) Ghouri, N.; Hippisley-Cox, J.; Newton, J.; Sheikh, A. Trends in the epidemiology and prescribing of medication for allergic rhinitis in England. *J. R. Soc. Med.* **2008**, *101*, 466–472.
- (3) Horak, F. VTX-1463, a novel TLR8 agonist for the treatment of allergic rhinitis. *Expert Opin. Invest. Drugs* **2011**, *20*, 981–986.
- (4) Di Capite, J. L.; Bates, G. J.; Parekh, A. B. Mast cell CRAC channel as a novel therapeutic target in allergy. *Curr. Opin. Allergy Clin. Immunol.* **2011**, *11*, 33–38.
- (5) Mandhane, S. N.; Shah, J. H.; Thennati, R. Allergic rhinitis: an update on disease, present treatments and future prospects. *Int. Immunopharmacol.* **2011**, *11*, 1646–1662.
- (6) Barnes, P. J. Drugs for asthma. *Br. J. Pharmacol.* **2006**, *147*, S297–S303.
- (7) McDonough, A. K.; Curtis, J. R.; Saag, K. G. The epidemiology of glucocorticoid associated adverse events. *Curr. Opin. Rheumatol.* **2008**, *20*, 131–137.
- (8) Schacke, H.; Docke, W. D.; Asadullah, K. Mechanisms involved in the side effects of glucocorticoids. *Pharmacol. Ther.* **2002**, *96*, 23–43.
- (9) Mullane, K. The increasing challenge of discovering asthma drugs. *Biochem. Pharmacol.* **2011**, *82*, 586–599.
- (10) Spataro, A. C.; Bosmann, H. B. Mechanism of action of disodium cromoglycate mast cell calcium-ion influx after a histamine releasing. *Biochem. Pharmacol.* **1976**, *25*, 505–510.
- (11) Abbas, A. K.; Lichtman, A. H.; Pillai, S. *Cellular and Molecular Immunology*, 6th ed.; Saunders Elsevier: Philadelphia, 2007.
- (12) Schwartz, L. B.; Austen, K. F. Enzymes of the mast cell granule. *J. Invest. Dermatol.* **1980**, *74*, 349–353.
- (13) Metcalfe, D. D.; Baram, D.; Mekori, Y. A. Mast cells. *Physiol. Rev.* **1997**, *77*, 1033–1079.
- (14) Klemm, S.; Ruland, J. Inflammatory signal transduction from the Fc epsilon RI to NF-kappaB. *Immunobiology* **2006**, *211*, 815–820.
- (15) Mazurek, N.; Bashkin, P.; Loyter, A.; Pecht, I. Restoration of Ca²⁺ influx and degranulation capacity of variant RBL-2H3 cells upon implantation of isolated cromolyn binding protein. *Proc. Natl. Acad. Sci. U.S.A.* **1983**, *80*, 6014–6018.
- (16) Mazurek, N.; Berger, G.; Pecht, I. A binding site on mast cells and basophils for the anti-allergic drug cromolyn. *Nature* **1980**, *286*, 722–723.
- (17) Foreman, J. C.; Garland, L. G. Cromoglycate and Other Antiallergic Drugs: A Possible Mechanism Of Action. *Brit. Med. J.* **1976**, *1*, 820–821.
- (18) Howell, J. B. L.; Altounyan, R. E. C. A double-blind trial of disodium cromoglycate in the treatment of allergic bronchial asthma. *Lancet* **1967**, *290*, 539–542.
- (19) Cairns, H.; Cox, J. S. G.; Minshull, R.; Fitzmaur, C.; Lord, G. H.; Lee, T. B.; King, J.; Johnson, P. B.; Hunter, D. Synthesis and structure–activity relationships of disodium cromoglycate and some related compounds. *J. Med. Chem.* **1972**, *15*, 583–589.
- (20) Portoghese, P. S.; Nagase, H.; MaloneyHuss, K. E.; Lin, C.-E.; Takemori, A. E. Role of Spacer and Address Components in Peptidomimetic δ Opioid Receptor Antagonists Related to Naltrindole. *J. Med. Chem.* **1991**, *34*, 1715–1720.
- (21) Beharry, A. A.; Woolley, G. A. Azobenzene photoswitches for biomolecules. *Chem. Soc. Rev.* **2011**, *40*, 4422–4437.
- (22) Vomasta, D.; Högnér, C.; Branda, N. R.; König, B. Regulation of Human Carbonic Anhydrase I (hCAI) Activity by Using a Photochromic Inhibitor. *Angew. Chem., Int. Ed.* **2008**, *40*, 7644–7647.
- (23) Stein, M.; Middendorp, S. J.; Carta, V.; Pejo, E.; Raines, D. E.; Forman, S. A.; Sigel, E.; Trauner, D. Azo-Propofols: Photochromic

Potentiators of GABA_A Receptors. *Angew. Chem., Int. Ed.* **20012**, *51*, 10500–10504.

(24) Mendonça, C. R.; Balogh, D. T.; De Boni, L.; dos Santos, D. S., Jr.; Zucolotto, V.; Oliveira, O. N., Jr. Optically Induced Processes in Azopolymers. In *Molecular Switches*, 2nd ed.; Feringa, B. L., Browne, W. R., Eds.; John Wiley & Sons: New York, 2011.

(25) Portoghese, P. S. Bivalent ligands and the message-address concept in the design of selective opioid receptor antagonists. *Trends Pharmacol. Sci.* **1989**, *10*, 230–235.

(26) Portoghese, P. S. From Models to Molecules: Opioid Receptor Dimers, Bivalent Ligands, and Selective Opioid Receptor Probes. *J. Med. Chem.* **2001**, *44*, 2259–2269.

(27) Walenzyk, T.; Carola, C.; Buchholz, H.; König, B. Chromone derivatives which bind to human hair. *Tetrahedron* **2005**, *61*, 7366–7377.

(28) Barker, G.; Ellis, G. P. Benzopyrones. Part I. 6-Amino- and 6-hydroxy-2-substituted chromones. *J. Chem. Soc., C* **1970**, 2230–2233.

(29) Wu, L.; Lal, J.; Simon, K. A.; Burton, E. A.; Luk, Y. Y. Nonamphiphilic Assembly in Water: Polymorphic Nature, Thread Structure, and Thermodynamic Incompatibility. *J. Am. Chem. Soc.* **2009**, *131*, 7430–7443.

(30) Bandara, H. M. D.; Burdette, S. C. Photoisomerization in different classes of azobenzene. *Chem. Soc. Rev.* **2012**, *41*, 1809–1825.

(31) Kirshenbaum, A. S.; Akin, C.; Wu, Y. L.; Rottem, M.; Goff, J. P.; Beaven, M. A.; Rao, V. K.; Metcalfe, D. D. Characterization of novel stem cell factor responsive human mast cell lines LAD 1 and 2 established from a patient with mast cell sarcoma/leukemia; activation following aggregation of Fc epsilon RI or Fc gamma RI. *Leuk. Res.* **2003**, *27*, 677–682.

(32) Passante, E.; Ehrhardt, C.; Sheridan, H.; Frankish, N. RBL-2H3 cells are an imprecise model for mast cell mediator release. *Inflammation Res.* **2009**, *58*, 611–618.

(33) Schwartz, L. B.; Austen, K. F.; Wasserman, S. I. Immunological release of beta-hexosaminidase and beta-glucuronidase from purified rat serosal mast cells. *J. Immunol.* **1979**, *123*, 1445–1450.

(34) Paton, W. D. M. Compound 48/80—a potent histamine liberator. *Brit. J. Pharm.* **1951**, *6*, 499–508.

(35) Shore, P. A.; Burkhalter, A.; Cohn, V. H. A method for the fluorometric assay of histamine in tissues. *J. Pharmacol. Exp. Ther.* **1959**, *127*, 182–186.

(36) Khandwala, A.; Vaninwegen, R.; Coutts, S.; Dallymeade, V.; Youssefyeh, R. D. Anti-allergic activity profile invitro of RHC-2963 and related compounds. *Int. J. Immunopharmacol.* **1983**, *5*, 491–502.

(37) Norris, A. A.; Alton, E. W. F. W. Chloride transport and the action of sodium cromoglycate and nedocromil sodium in asthma. *Clin. Exp. Allergy* **1996**, *26*, 250–253.

(38) Yang, Y. H.; Lu, J. Y. L.; Wu, X. S.; Summer, S.; Whoriskey, J.; Saris, C.; Reagan, J. D. G-Protein-Coupled Receptor 35 Is a Target of the Asthma Drugs Cromolyn Disodium and Nedocromil Sodium. *Pharmacology* **2010**, *86*, 1–5.

(39) Samanta, S.; Qin, C.; Lough, A. J.; Woolley, G. A. Bidirectional Photocontrol of Peptide Conformation with a Bridged Azobenzene Derivative. *Angew. Chem., Int. Ed.* **2012**, *51*, 6452–6455.

(40) Szymanski, W.; Wu, B.; Poloni, C.; Janssen, D. B.; Feringa, B. L. Azobenzene Photoswitches for Staudinger–Bertozzi Ligation. *Angew. Chem., Int. Ed.* **2013**, *52*, 2068–2072.

(41) Bléger, D.; Schwarz, J.; Brouwer, A. M.; Hecht, S. *o*-Fluoroazobenzenes as Readily Synthesized Photoswitches Offering Nearly Quantitative Two-Way Isomerization with Visible Light. *J. Am. Chem. Soc.* **2012**, *134*, 20597–20600.

(42) Szymanki, W.; Beierle, J. M.; Kistemaker, H.; Velema, W. A.; Feringa, B. L. Reversible Photocontrol of Biological Systems by the Incorporation of Molecular Photoswitches. *Chem. Rev.* DOI:10.1021/cr300179f.

(43) Zhu, D.; Lu, M.; Chua, P. J.; Tan, B.; Wang, F.; Yang, X.; Zhong, G. A Highly Stereoselective Organocatalytic Tandem Aminoylation/Aza Michael Reaction for the Synthesis of Tetrahydro-1,2-Oxazines. *Org. Lett.* **2008**, *10*, 4585–4588.

(44) Sakamoto, R.; Murata, M.; Kume, S.; Sampei, H.; Sugimoto, M.; Nishihara, H. Photo-controllable tristability of a dithiolato-bipyridine-Pt(II) complex molecule containing two azobenzene moieties. *Chem. Commun.* **2005**, 1215–1217.

(45) Joussetme, B.; Blanchard, P.; Gallego-Planas, N.; Levillain, E.; Delaunay, J.; Allain, M.; Richomme, P.; Roncali, J. Photomechanical Control of the Electronic Properties of Linear π Conjugated Systems. *Chem–Eur. J.* **2003**, *9*, 5297–5306.

(46) Bonardi, F.; London, G.; Nouwen, N.; Feringa, B.; Driessen, A. J. M. Light-Induced Control of Protein Trans location by the SecYEG Complex. *Angew. Chem., Int. Ed.* **2010**, *49*, 7234–7238.